AMERICAN SOCIETY FOR MICROBIOLOGY | Molecular and Cellular Biology®

RESEARCH ARTICLE

# P-Body Localization of the Hrr25/Casein Kinase 1 Protein Kinase Is Required for the Completion of Meiosis

**Bo Zhang,[a] Anna M. Butler,[a] Qian Shi,[a] Siyuan Xing,[a] Paul K. Herman[a]**

[a]Department of Molecular Genetics, The Ohio State University, Columbus, Ohio, USA

**ABSTRACT** P-bodies are liquid droplet-like compartments that lack a limiting membrane and are present in many eukaryotic cells. These structures contain specific sets of proteins and mRNAs at concentrations higher than that in the surrounding environment. Although highly conserved, the normal physiological roles of these ribonucleoprotein (RNP) granules remain poorly defined. Here, we report that P-bodies are required for the efficient completion of meiosis in the budding yeast *Saccharomyces cerevisiae*. P-bodies were found to be present during all phases of the meiotic program and to provide protection for the Hrr25/CK1 protein kinase, a key regulator of this developmental process. A failure to associate with these RNP granules resulted in diminished levels of Hrr25 and an ensuing inability to complete meiosis. This work therefore identifies a novel function for these RNP granules and indicates how protein recruitment to these structures can have a significant impact on eukaryotic cell biology.

**KEYWORDS** CK1 protein kinase, meiosis, membraneless organelles, P-bodies, sporulation

The eukaryotic cell is divided into distinct functional domains by a collection of membrane-bound organelles that includes the nucleus, endoplasmic reticulum, and mitochondria. However, it is becoming increasingly clear that the nucleoplasm and remaining cytoplasm are further subdivided into a variety of additional compartments that lack a limiting membrane (1, 2). These "membraneless" organelles include the long-studied nucleolus and centrosome, as well as the more recently identified RNA-protein (RNP) granules, like the processing body (P-body) and stress granule (3). These membraneless compartments tend to be relatively dynamic structures that are able to assemble (or disassemble) rapidly in response to the appropriate environmental cues. These structures have been conserved through evolutionary time, and several have been linked to a number of human disorders, including particular neurodegenerative conditions (2, 4–7). It is therefore imperative that we identify their normal physiological roles in the cell.

The P-body is a cytoplasmic RNP granule that is present in all eukaryotes examined to date, from yeast to humans (8, 9). These RNP structures were originally defined by the presence of translationally arrested mRNAs and a number of proteins involved in mRNA processing, including the Dcp1/Dcp2 decapping complex and the Xrn1 5′ to 3′ exonuclease (10–14). These observations led to the suggestion that P-bodies are sites of mRNA decay in the cell (15, 16). However, more recent work indicates that mRNA turnover likely is not occurring in P-body granules. For example, no significant defects in mRNA decay were observed in yeast or mammalian cells lacking P-body foci (17–19). Moreover, studies with yeast decapping mutants suggest that mRNA turnover is actively suppressed within the P-body proper (20, 21). As a result, the biological functions associated with these RNP structures remain to be determined.

P-bodies, and other RNP granules, have also been found to contain a variety of

**Received** 28 December 2017 **Returned for modification** 2 February 2018 **Accepted** 12 June 2018

**Accepted manuscript posted online** 18 June 2018

**Citation** Zhang B, Butler AM, Shi Q, Xing S, Herman PK. 2018. P-body localization of the Hrr25/casein kinase 1 protein kinase is required for the completion of meiosis. Mol Cell Biol 38:e00678-17. https://doi.org/10.1128/MCB.00678-17.



Address correspondence to Paul K. Herman, herman.81@osu.edu.

signaling molecules important for the proper control of cell proliferation and survival (22–29). This list includes a number of essential protein kinases and phosphatases in both mammalian and yeast cells. These findings have led researchers to propose that these RNP granules could have a role in the rewiring of cellular signaling networks under specific conditions of stress (25, 30, 31). Work from our laboratory has shown that the Hrr25 protein kinase is efficiently localized to P-bodies under all conditions tested in the yeast *Saccharomyces cerevisiae* (25, 31). Hrr25 is an essential enzyme and is the yeast ortholog of the $\delta/\varepsilon$ isoforms of the mammalian CK1 protein kinase (32). Hrr25/CK1 enzymes have been shown to have conserved roles in ribosome maturation, vesicle trafficking, DNA repair, clathrin-mediated endocytosis, and meiosis (33–42). The association with P-body granules is also evolutionarily conserved, as the human CK1$\delta$ enzyme was detected within P-body foci in HeLa cells (31). In yeast, this P-body localization has been shown to be important for the maintenance of the normal cellular levels of Hrr25 by shielding this protein from degradation by the proteasome (31). However, the physiological significance of this protection had not yet been demonstrated.

In this report, we show that the P-body localization of Hrr25 is necessary for the efficient completion of the meiotic program in *S. cerevisiae*. Although these RNP granules had been shown to form under a variety of stress conditions, it was not known if they were present or required during such developmental transitions. The data here demonstrate that P-bodies are indeed present in cells undergoing meiosis and suggest that these RNP structures are required for the completion of this developmental process. In all, this work identifies a novel function for these RNP granules and indicates how protein recruitment to these foci can have a significant impact on eukaryotic cell biology.

## RESULTS AND DISCUSSION

**P-body granules are present in meiotic cells.** To determine if P-bodies were induced in cells undergoing meiosis, we used diploid strains expressing green fluorescent protein (GFP)-tagged versions of known protein constituents of P-body foci. These reporters included Dcp1 and Dcp2, the regulatory and catalytic subunits of the mRNA decapping enzyme, Edc3, an enhancer of mRNA decapping, Pat1, a scaffolding protein, Dhh1, a DEAD box RNA helicase, and Xrn1 (13). We found that P-body foci were induced following the transfer to prespore growth medium and that these granules persisted throughout the sporulation process (Fig. 1A and B and 2A). Yeast meiosis results in the production of four haploid spore progeny and is referred to as sporulation (43). The fraction of cells containing GFP foci was greater than 90% for all times examined for both Dcp2 and Edc3 (Fig. 1C and D). Similar results were obtained with the other P-body reporters tested. Therefore, P-bodies are present in cells undergoing meiosis, and these granules contain the known markers for these membraneless organelles. It should be pointed out that the induction of sporulation involves a transfer to a growth medium that lacks glucose, a condition known to induce P-body foci in *S. cerevisiae*. Whether P-bodies are generally induced during meiosis in other organisms is a question that remains to be answered.

The morphology and number of P-body foci were observed to change as cells progressed through the meiotic program. Specifically, these foci became smaller and more numerous as meiosis proceeded. Cells in prespore medium generally had one, or perhaps two, larger foci that were reminiscent of what is observed in cells deprived of glucose or exposed to oxidative stress (44, 45). In the latter instances, the larger P-body foci typically persist for the duration of the stress (31). However, we found here that the number of foci increased during meiosis until it reached a maximum of approximately six per cell (Fig. 1E and F). The foci at these later times were generally smaller and less fluorescent than those initially observed during growth in the prespore medium. A potential explanation for these observations is that P-bodies undergo a process of fission during the early stages of meiotic development that facilitates more equal partitioning of granule constituents between the newly forming spores.

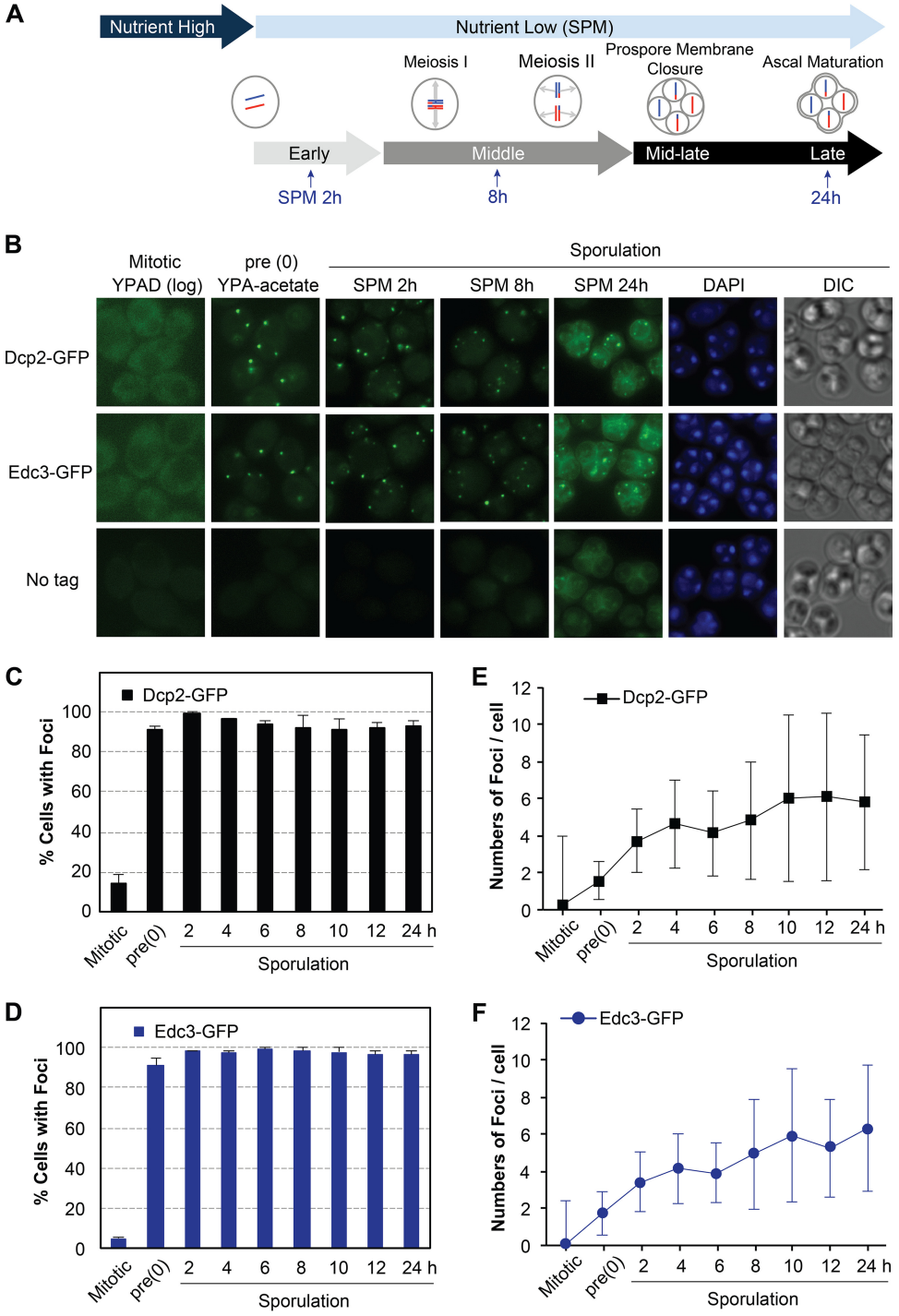


**FIG 1** P-bodies are present in meiotic cells. (A) A schematic showing the major events of meiosis (43). (B) Time course of P-body formation during meiosis. Cells expressing the P-body reporter Dcp2 or Edc3-GFP were grown to mid-log phase in rich medium (YPAD) and then subjected to the sporulation regimen described in Materials and Methods. P-body formation was assessed by fluorescence microscopy at the indicated times. Spore formation was assessed by observing cells in the differential interference contrast (DIC) channel after staining their DNA with the fluorescent stain DAPI. Cells with no GFP reporter (no tag) served as a control for the autofluorescence that was observed with sporulating cells. (C and D) The percentage of cells with Dcp2- or Edc3-GFP foci was determined at each of the indicated time points. (E and F) The average number of Dcp2- or Edc3-GFP foci per cell was assessed at each of the indicated time points.

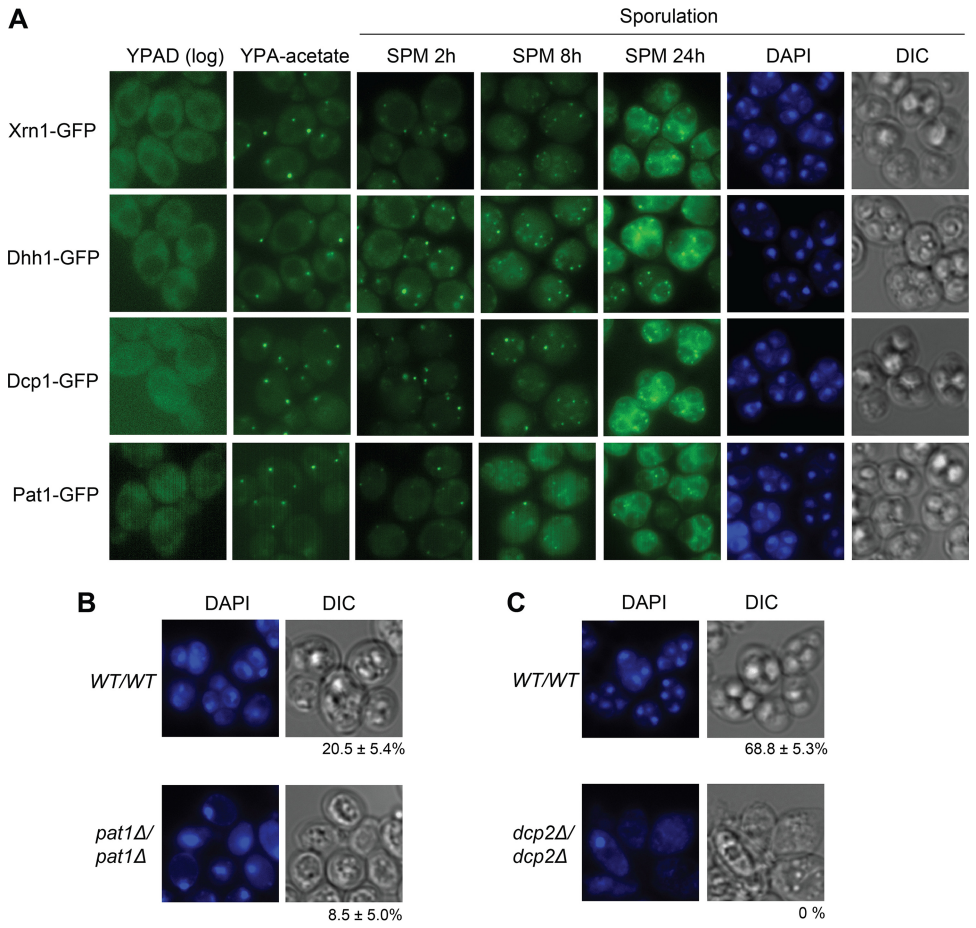


**FIG 2** P-body proteins Pat1 and Dcp2 are required for an efficient meiosis. (A) An analysis of P-body composition during meiosis. Cells expressing the additional P-body reporters Xrn1-, Dhh1-, Dcp1-, or Pat1-GFP were grown to mid-log phase in rich medium (YPAD) and then subjected to the sporulation regimen described in Materials and Methods. P-body formation was assessed by fluorescence microscopy at the indicated times. Spore formation was assessed by observing cells in the DIC channel after staining their DNA with the fluorescent stain DAPI. (B and C) Sporulation was defective in diploid cells lacking the P-body component Pat1 (B) or Dcp2 (C). The sporulation efficiency of the indicated diploid strains was assessed as described in Materials and Methods. Note that the difference in sporulation efficiency between the two wild-type strains was due to their different genetic backgrounds.

**Alterations of P-body composition affect meiotic efficiency.** To test whether P-body integrity was important for meiosis, we examined the sporulation of diploid strains lacking either the Pat1 or Dcp2 protein. Pat1 is a key scaffolding protein required for efficient P-body formation, and *pat1*Δ cells have a diminished ability to form P-body foci (46–48). In contrast, Dcp2 is not required for P-body assembly *per se* but is necessary for the recruitment of the Hrr25 protein kinase to these RNP granules (31, 47). We found that sporulation efficiency was significantly reduced in both *pat1*Δ/*pat1*Δ and *dcp2*Δ/*dcp2*Δ mutants (Fig. 2B and C). Very few four-spore asci were observed with either strain. Together these results are consistent with P-bodies having an important role during the sporulation process. In particular, the defects observed in the *dcp2*Δ/*dcp2*Δ mutant could be due to the decreased level of mRNA decapping activity associated with this strain or to the absence of Hrr25 in the remaining P-body foci. Here, we examined the contribution of the latter phenomenon to the meiotic program.

**The Hrr25/CK1 protein kinase is efficiently recruited to P-body foci at specific stages of the meiotic program.** To assess P-body localization, we examined yeast strains that expressed GFP-tagged versions of either the wild-type Hrr25 or the Hrr25$^{PLS1*}$ variant that is defective for P-body localization (31). The latter variant has two alterations within P-body localization signal 1 (PLS1), R294A and K297A, that disrupt its

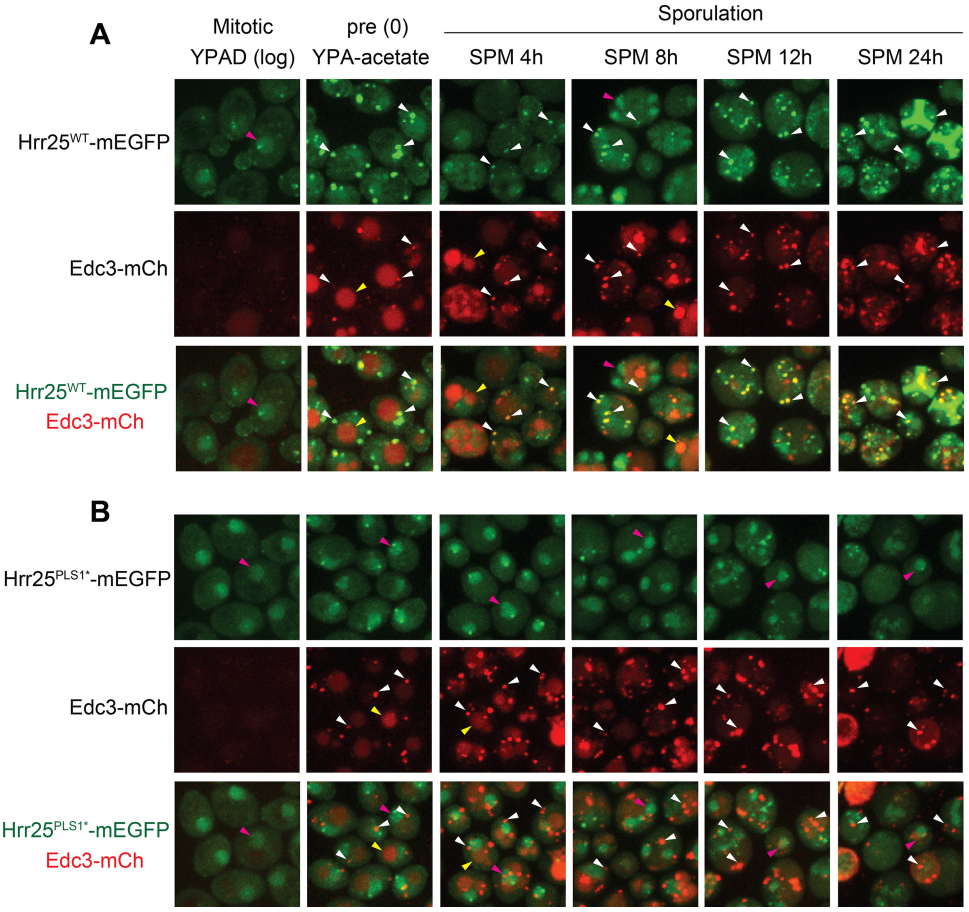


**FIG 3** Hrr25 was associated with P-bodies in meiotic cells. (A and B) Strains expressing the P-body reporter Edc3-mCh and either the wild-type Hrr25 (A) or the Hrr25$^{PLS1*}$ variant (B) were examined by fluorescence microscopy at the indicated phases of the meiotic program. SPM, sporulation medium. The merged images are shown in the third row in each case. The white arrowheads indicate P-body foci, magenta arrowheads indicate nuclei with Hrr25-GFP at the spindle pole body, and yellow arrowheads identify instances of autofluorescence.

normal interaction with Dcp2. This association with Dcp2 is required for the recruitment of Hrr25 to P-body granules. Here, we found that the wild-type Hrr25, but not the Hrr25$^{PLS1*}$ variant, was localized to cytoplasmic foci in cells undergoing meiosis (Fig. 3). During growth in the prespore medium, these foci generally corresponded to P-bodies, as there was greater than 80% colocalization between Hrr25 and an Edc3-mCh reporter. In contrast, there was very little colocalization observed at this time between Edc3 and the Hrr25$^{PLS1*}$ variant. The Hrr25 foci that are associated with the nucleus are very likely identifying the spindle pole body, a structure that Hrr25 is also associated with in yeast cells (Fig. 3) (31, 49). In addition, the large, red circular structures observed in the premeiotic cells are the result of autofluorescence from the vacuolar compartment; this signal is independent of the Edc3-mCh reporter. Altogether, these data suggest that Hrr25 is recruited to P-body foci in meiotic cells in a manner that is also dependent upon its interaction with Dcp2.

Hrr25 localization was also assessed by fluorescence microscopy at different stages of the meiotic program (Fig. 4A). These analyses indicated that Hrr25 was strongly associated with P-bodies both before and after the two meiotic divisions that characterize this developmental process. However, this association was less pronounced in cells that appeared to be undergoing nuclear separation during either meiosis I or II (Fig. 4B). The latter cells were marked by the presence of the Hrr25-GFP fusion within the dividing nuclei. The fraction of Edc3-containing foci that also contained Hrr25-GFP dropped from greater than 80% during growth in the prespore medium to almost 20%

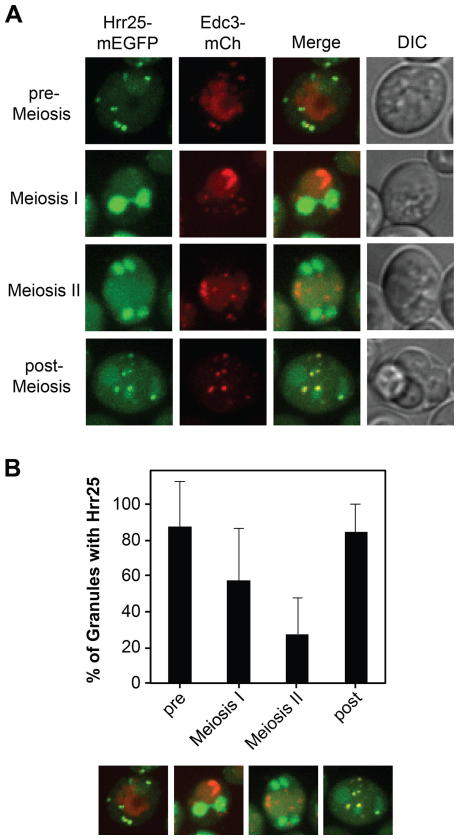


**FIG 4** Hrr25 localization to P-bodies was diminished as cells underwent meiotic divisions I and II. (A) Images of individual cells expressing Hrr25-mEGFP and Edc3-mCh at the indicated stages of the meiotic program are shown. (B) The graph shows the fraction of Edc3 foci that also contain Hrr25 in cells at the indicated stage of meiosis. At least 30 cells for two independent isolates of the tagged strain were analyzed for each of the indicated stages of the meiotic program.

in cells undergoing meiotic division II. At later times, the colocalization between Hrr25 and Edc3 was back to ~80% (Fig. 4, postmeiosis). These data are therefore consistent with Hrr25 being present in P-bodies prior to the two meiotic divisions and then migrating into the nucleus during meiosis I and II. The potential significance of this observation is discussed below.

**Hrr25 association with P-bodies may be required for the efficient completion of meiosis.** To test whether the P-body localization of Hrr25 is important for meiosis, we assessed the sporulation efficiency of a diploid strain that expressed only the Hrr25$^{PLS1*}$ variant (referred to here as *PLS1*/PLS1**). We found that this strain exhibited a severe defect in the completion of meiosis with two independent assays. In the first, we directly assessed spore formation by microscopy and observed a greater than 20-fold decrease in sporulation efficiency (Fig. 5A and B). The second method employed a growth-based plating assay that measures the ability of the diploid to generate haploid progeny with a specific genotype. Briefly, the diploid strains used here express the *Schizosaccharomyces pombe his5*$^{+}$ gene from the haploid-specific promoter of the *S. cerevisiae STE2* gene (50). *STE2* encodes the $\alpha$-factor pheromone receptor and is expressed only in *MAT***a** haploid cells. The assay thus assesses the ability to produce *MAT***a** cell progeny that would be able to grow on the selective plates that lack exogenous histidine (see Materials and Methods for further details). Using this plating assay, we observed a very severe sporulation defect with the *PLS1*/PLS1** strain, as it produced at least 500-fold fewer viable haploid progeny than the isogenic wild-type control (Fig. 5C). Thus, the P-body localization of Hrr25 may be important for the effective completion of the meiotic program.

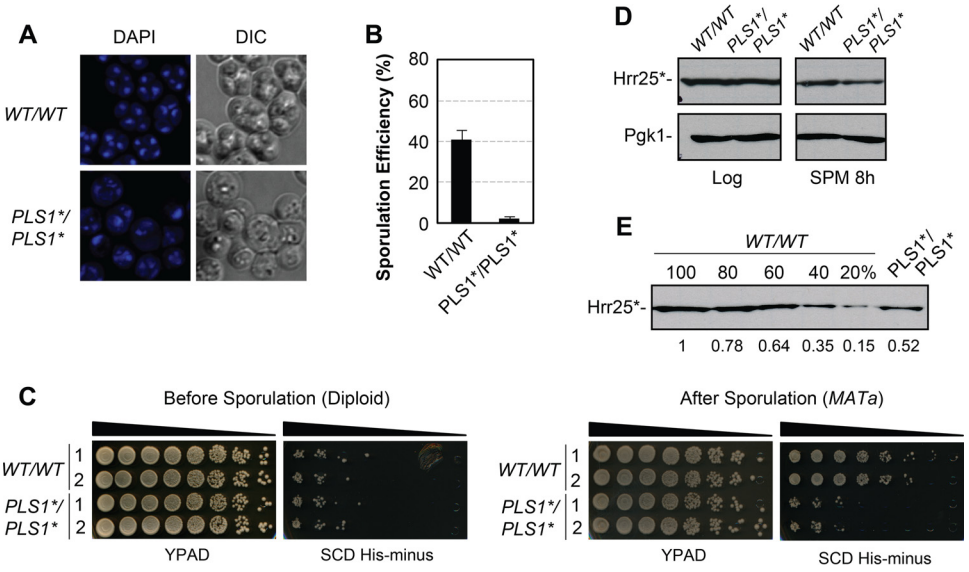


**FIG 5** Cells expressing the Hrr25$^{PLS1*}$ variant have diminished levels of the Hrr25 protein and exhibit a decreased level of sporulation. (A and B) Strains expressing the Hrr25$^{PLS1*}$ variant exhibited a decreased level of sporulation. The indicated strains were incubated in sporulation medium for 24 h as described in Materials and Methods, and the efficiency of the sporulation process was determined by microscopy. Representative images are shown in panel A, and the quantitation of the data is presented in panel B. (C) A plate assay was used to assess the level of sporulation in diploids expressing either the wild-type Hrr25 (*WT/WT*) or the Hrr25$^{PLS1*}$ variant (*PLS1*/PLS1**) that fails to associate with P-bodies. The relative number of haploid progeny formed is indicated by the number of colonies forming on the selective medium, SCD His-minus. See Materials and Methods for more details. (D and E) The levels of the Hrr25$^{PLS1*}$ variant were approximately 2-fold lower than that of the wild-type protein in sporulating cells. The levels of the wild-type Hrr25 and the Hrr25$^{PLS1*}$ variant were determined with a Western blot analysis of extracts prepared from log-phase and sporulating cells, as indicated. In panel E, differing amounts of the *WT/WT* protein extract were used to identify the relative level of the Hrr25$^{PLS1*}$ variant in the *PLS1*/PLS1** diploid. Quantitation of the relative amounts of Hrr25 present in each sample is indicated by the numbers below the blot.

**The localization to P-bodies ensures that a critical level of Hrr25 is available to meiotic cells.** Our prior work demonstrated that the P-body association of Hrr25 during periods of stress served to protect this protein from degradation by the proteasome (31). Therefore, we tested here whether this granule association has a similar protective effect during meiosis. Specifically, we asked whether there were lower levels of the Hrr25$^{PLS1*}$ variant in cells that were undergoing meiosis. A Western blot analysis determined that the level of the Hrr25$^{PLS1*}$ variant was approximately 50% of that of the wild-type protein after 8 h of sporulation (Fig. 5D and E). Therefore, the association with the P-body during the early stages of meiosis may allow the cell to maintain a critical level of Hrr25 that is necessary for the subsequent completion of this developmental program.

If the meiotic defect in the *PLS1*/PLS1** strain was due to the lower level of Hrr25 protein, we reasoned that it should be possible to phenocopy this effect by decreasing the level of the wild-type Hrr25 in diploid cells. Toward this end, we analyzed Hrr25 protein levels in a heterozygous diploid where one copy of the *HRR25* locus was deleted. The level of Hrr25 in this strain was found to be 50 to 60% of that observed in the homozygous wild-type diploid, a level similar to that detected in the *PLS1*/PLS1** strain (Fig. 6A). We therefore assessed the sporulation efficiency of this heterozygous strain and found that it was significantly reduced relative to that of the wild type (Fig. 6B and C). In fact, there were almost no four-spore meioses observed with the *HRR25/−* diploid. These observations indicate that meiotic cells are very sensitive to the levels of Hrr25 protein and that a reduction by 2-fold has a significant negative effect on the ability to complete the meiotic program. Finally, this model also predicts that the meiotic defect associated with the *PLS1*/PLS1** diploid would be suppressed by restoring the levels of the Hrr25$^{PLS1*}$ variant. Therefore, we introduced a plasmid that had this variant locus under the control of the copper-inducible promoter from the *CUP1* gene.

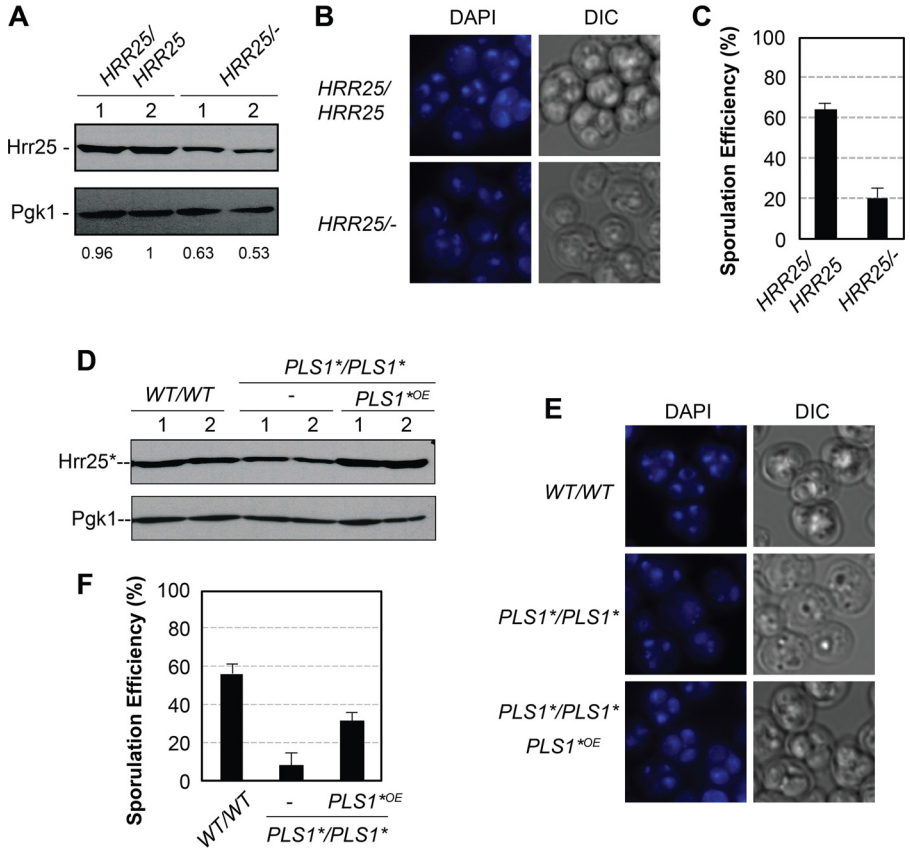


**FIG 6** The *HRR25* locus is haploinsufficient with respect to sporulation. (A) A Western blot analysis showed that Hrr25 levels in a *HRR25/hrr25*Δ heterozygous diploid were approximately one-half of that detected in a homozygous wild-type diploid. (B and C) Sporulation efficiency was significantly decreased in a *HRR25/hrr25*Δ heterozygous diploid strain. The indicated strains were incubated in sporulation medium for 24 h, and the efficiency of the sporulation process was assessed with a microscopy-based assay. Representative images are shown in panel B, and the quantitation of the data is presented in panel C. (D) Hrr25 protein levels in the indicated strains were assessed with a Western blot analysis after 6 h in sporulation medium. PLS1$^{*OE}$ indicates the presence of a plasmid that results in the overexpression of the Hrr25$^{PLS1*}$ variant. Quantitation of the blot found that the levels of Hrr25$^{PLS1*}$ in the overexpression strains were 1.12× and 1.55× relative to those of the wild-type controls. (E and F) The sporulation defect associated with the *PLS1*/PLS1** diploid strain was partially suppressed by restoring the expression levels of the Hrr25$^{PLS1*}$ variant.

Using this construct, we found that the expression of Hrr25$^{PLS1*}$ at levels 1.12 or 1.55 times that of the wild-type protein was able to partially restore sporulation in the *PLS1*/PLS1** strain (Fig. 6E and F). These results are therefore consistent with the sporulation defect in the *PLS1*/PLS1** diploid being due, at least in part, to the diminished levels of the Hrr25$^{PLS1*}$ present in this strain.

**Examining the activities of the Hrr25$^{PLS1*}$ variant.** Hrr25 is an essential protein kinase that has conserved roles in a number of processes in dividing cells. In a previous study, we showed that the alterations associated with the Hrr25$^{PLS1*}$ variant did not have a significant effect on these mitotic activities (31). Yeast cells expressing only this variant exhibit a growth rate very similar to that of wild-type cells. Here, we extended this analysis and found that cells with this variant also exhibited a normal response to the DNA-damaging agent methyl methanesulfonate (MMS) (Fig. 7A). In contrast, mutants with diminished Hrr25 kinase activity exhibited a greatly increased sensitivity to this chemical agent (Fig. 6A) (33, 51). Altogether, these data are consistent with the Hrr25$^{PLS1*}$ variant functioning like the wild-type protein in mitotic cells.

Hrr25 is also known to be important for several steps of the meiotic program (34, 40, 52). In particular, Hrr25 appears to phosphorylate the Rec8 cohesion subunit and to be a component of the budding yeast monopolin complex important for sister kineto-

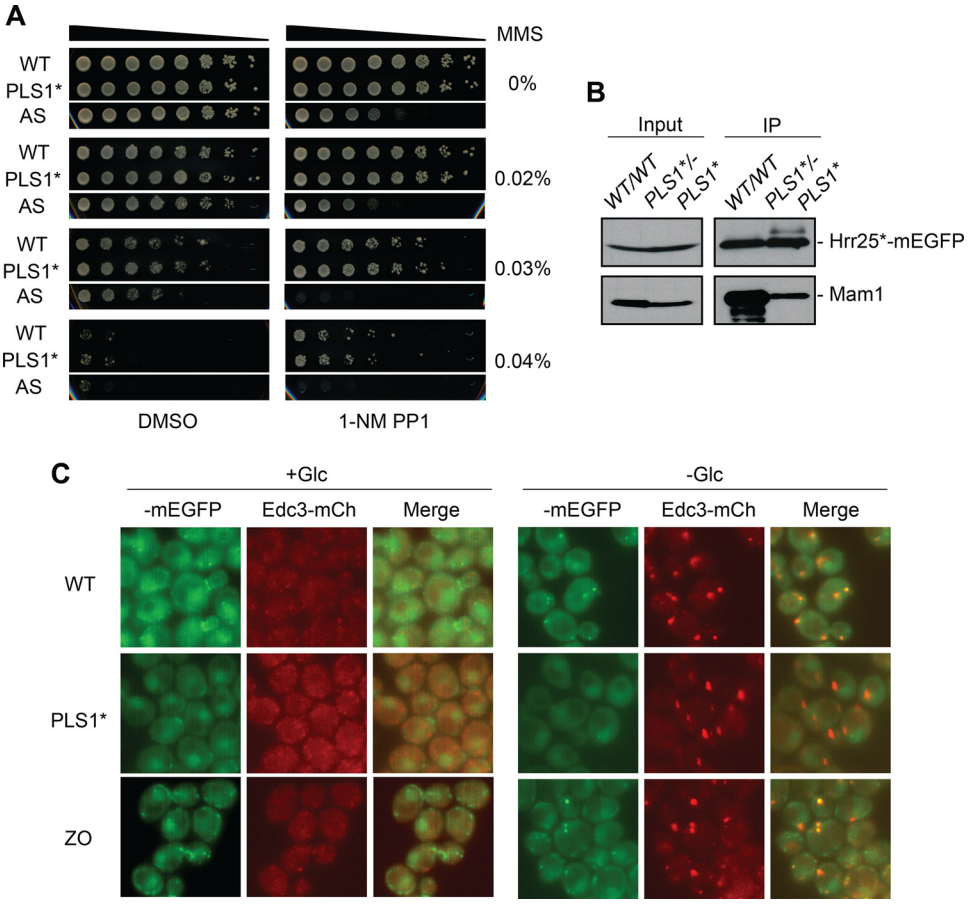


**FIG 7** Analysis of the mitotic and meiotic functions associated with Hrr25. (A) The Hrr25$^{PLS1*}$ variant is functional in DNA repair. Yeast strains expressing the indicated versions of Hrr25 were grown to mid-log phase in SCD minimal medium before being plated onto the same medium containing the indicated concentrations of the DNA-damaging agent MMS. For plating, the cells were resuspended in water at a final concentration of 10 $OD_{600}$ equivalents/ml, and 5 $\mu$l of this cell suspension and 5-fold serial dilutions thereafter were applied to the plates. The drug 1-NM PP1 was added where indicated to inhibit the protein kinase activity of the analog-sensitive version of Hrr25 (AS). (B) The Hrr25 interaction with the Mam1 protein. An immunoprecipitation (IP) assay was used to assess the interaction between Mam1 and the Hrr25$^{PLS1*}$ variant. Protein samples were prepared from the indicated diploid strains following 8 h in SPM, and the Hrr25-mEGFP proteins were precipitated with an antibody specific for the GFP tag. The amount of associated Mam1-13Myc protein was then detected by Western blotting with an antibody specific for the myc epitope. (C) The Hrr25$^{ZO}$ variant is efficiently localized to P-body foci. Cells expressing the indicated variants of the Hrr25 protein were analyzed by fluorescence microscopy before (+Glc) and 15 min after (−Glc) transfer to a medium lacking glucose. Edc3-mCherry was used as a reporter for P-body foci.

chore coorientation during meiosis I (34, 40, 53, 54). With respect to the latter, Hrr25 interacts with Mam1, a second component of this four-protein complex, and this interaction appears to be necessary for accurate chromosome segregation (34). Structural analyses indicate that residues from the kinase and central domains of Hrr25 are involved in an extensive interface with Mam1 (55). The residues altered in the Hrr25$^{PLS1*}$ variant are within these domains, and we therefore examined the Hrr25$^{PLS1*}$ protein interaction with Mam1. Using an immunoprecipitation approach, we found that Hrr25$^{PLS1*}$ was partially defective for this interaction (Fig. 7B). The effects we observe here on sporulation could therefore be due to a failure of Hrr25$^{PLS1*}$ to associate with the P-body and/or to interact normally with Mam1.

To examine these possibilities further, we tested whether a previously identified Hrr25 variant that is defective for the interaction with Mam1 was able to associate with P-body foci. This variant, Hrr25-zo, is altered at two positions within the kinase domain, H25R and E34K (34). Interestingly, we found that Hrr25-zo was localized to P-bodies as efficiently as the wild-type Hrr25 protein (Fig. 7C). The colocalization with an Edc3-mCh

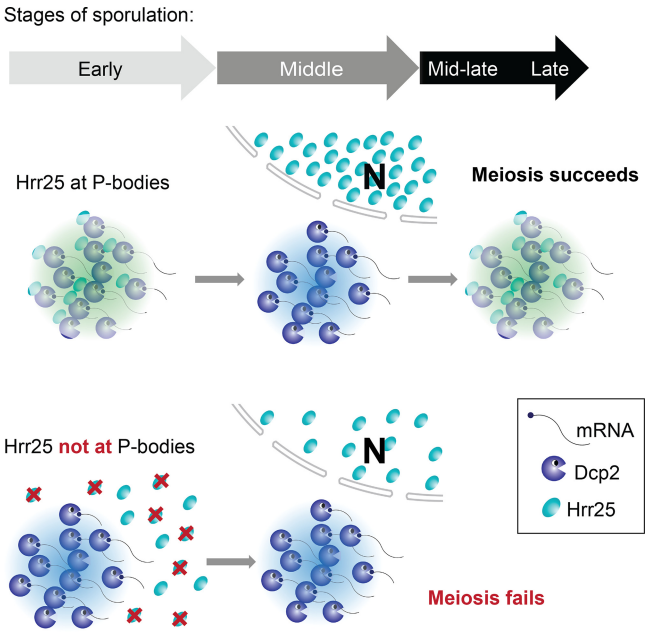


**FIG 8** Model describing the role of Hrr25 localization to the P-body during meiosis. The data here suggest that Hrr25 association with the P-body during the earliest stages of meiosis allows this protein to avoid degradation within the proteasome. This allows the cell to maintain a critical level of Hrr25 that is required during meiotic divisions I and II. During these divisions, a significant level of Hrr25 appears to be present in the nuclear compartment. A failure to associate with the P-body, like that observed with the Hrr25$^{PLS1*}$ variant, results in diminished levels of Hrr25 and a subsequent inability to complete the meiotic program.

reporter was found to be 81.7% for Hrr25-zo and 80.7% for the wild-type protein. Moreover, this Hrr25-zo variant has been shown to be present at wild-type levels in sporulating cells (34). Therefore, a failure to interact with Mam1 does not necessarily result in diminished levels of the Hrr25 protein. Instead, the observed decrease in Hrr25$^{PLS1*}$ levels is more likely due to the failure of this variant to associate with P-body granules. Since our data clearly demonstrate that a 2-fold decrement in Hrr25 levels results in a failure to complete the meiotic program, we feel that the P-body association of Hrr25 is likely to be important for an efficient meiosis. Specifically, we propose that this association allows the cell to maintain a critical level of Hrr25 that is necessary for the completion of meiosis.

**Summary.** The work here demonstrates that P-bodies are present in cells undergoing meiosis and that these RNP granules are important for the efficient completion of this developmental program. The latter requirement appears to be due, at least in part, to the ability of P-bodies to shield the Hrr25 protein kinase from the degradative machinery present in the cell. A failure to associate with the P-body results in diminished levels of Hrr25 that are unable to sustain meiosis. Our results support a model whereby Hrr25 associates with P-bodies during the earliest stages of meiosis in order to maintain the critical level of this enzyme that is needed during the ensuing meiotic divisions (Fig. 8). At the latter times, Hrr25 appears to be present in the nucleus, where it would be able to phosphorylate its nuclear targets. Following the completion of the second meiotic division, Hrr25 appears to associate again with the P-bodies present in the cytoplasm. It is not yet clear how this reversible association with the P-body is regulated, and addressing this issue will be a major focus of future studies. In all, we feel that the work here identifies a novel role for P-bodies during meiosis and demonstrates how protein recruitment to these RNP granules can have significant impact on the overall physiology of the eukaryotic cell.

## MATERIALS AND METHODS

**Yeast strains and plasmids.** Yeast strains used in this study are listed in Table 1. Most strains were constructed by introducing PCR-based gene deletions or mutant alleles as described previously (56).

**TABLE 1** Yeast strains used in this study[a]

| Strain | Genotype | Reference/source |
|---|---|---|
| PHY9661 | (BY) *MAT***a** *his3Δ1 leu2Δ0 met15Δ0 ura3Δ0*/(SK1) *MATα ura3 leu2 trp1 his3 arg4 lys2 hoΔ::LYS2 rme1Δ::LEU2* (no-tag control strain) | This study |
| PHY9871 | (BY) *MAT***a** *his3Δ1 leu2Δ0 met15Δ0 ura3Δ0* ***DCP2-GFP****::HIS3*/(SK1) *MATα ura3 leu2 trp1 his3 arg4 lys2 hoΔ::LYS2 rme1Δ::LEU2* | This study |
| PHY9881 | (BY) *MAT***a** *his3Δ1 leu2Δ0 met15Δ0 ura3Δ0* ***EDC3-GFP****::HIS3*/(SK1) *MATα ura3 leu2 trp1 his3 arg4 lys2 hoΔ::LYS2 rme1Δ::LEU2* | This study |
| PHY9873 | (BY) *MAT***a** *his3Δ1 leu2Δ0 met15Δ0 ura3Δ0* ***XRN1-GFP****::HIS3*/(SK1) *MATα ura3 leu2 trp1 his3 arg4 lys2 hoΔ::LYS2 rme1Δ::LEU2* | This study |
| PHY9875 | (BY) *MAT***a** *his3Δ1 leu2Δ0 met15Δ0 ura3Δ0* ***DHH1-GFP****::HIS3*/(SK1) *MATα ura3 leu2 trp1 his3 arg4 lys2 hoΔ::LYS2 rme1Δ::LEU2* | This study |
| PHY9877 | (BY) *MAT***a** *his3Δ1 leu2Δ0 met15Δ0 ura3Δ0* ***DCP1-GFP****::HIS3*/(SK1) *MATα ura3 leu2 trp1 his3 arg4 lys2 hoΔ::LYS2 rme1Δ::LEU2* | This study |
| PHY10446 | (BY) *MAT***a** *his3Δ1 leu2Δ0 met15Δ0 ura3Δ0* ***PAT1-GFP****::HIS3*/(SK1) *MATα ura3 leu2 trp1 his3 arg4 lys2 hoΔ::LYS2 rme1Δ::LEU2* | This study |
| PHY8596 | (BY) *MAT***a** *his3Δ1 leu2Δ0 met15Δ0 ura3Δ0*/(BY) *MATα his3Δ1 leu2Δ0 lys2Δ0 ura3Δ0* (wild type for PHY8837) | This study |
| PHY8837 | (BY) *MAT***a** *his3Δ1 leu2Δ0 met15Δ0 ura3Δ0* ***pat1****::**KAN***/(BY) *MATα his3Δ1 leu2Δ0 lys2Δ0 ura3Δ0* ***pat1****::**KAN*** | This study |
| PHY8690 | *MAT***a** *leu2-3.112 trp1 ura3-52 his4-539 cup1::LEU2/PGK1pG/MFA2pG DHH1-GFP* (*NEO*)/(BY) *MATα his3Δ1 leu2Δ0 lys2Δ0 ura3Δ0* (wild type for PHY8694) | This study |
| PHY8694 | *MAT***a** *leu2-3.112 trp1 ura3-52 his4-539 cup1::LEU2/PGK1pG/MFA2pG* ***dcp2****::**TRP1*** *DHH1-GFP* (*NEO*)/(BY) *MATα his3Δ1 leu2Δ0 lys2Δ0 ura3Δ0* ***dcp2****::**LEU2*** | This study |
| PHY9381 | (BY) *MAT***a** *his3Δ1 leu2Δ0 met15Δ0 ura3Δ0 HRR25-mEGFP::HIS3 EDC3-mCherry::LEU2*/(SK1) *MATα ura3 leu2 trp1 his3 arg4 lys2 hoΔ::LYS2 rme1Δ::LEU2 HRR25-mEGFP::HIS3* | This study |
| PHY9384 | (BY) *MAT***a** *his3Δ1 leu2Δ0 met15Δ0 ura3Δ0 HRR25$^{PLS1*}$-mEGFP::HIS3 EDC3-mCherry::LEU2*/(SK1) *MATα ura3 leu2 trp1 his3 arg4 lys2 hoΔ::LYS2 rme1Δ::LEU2 HRR25$^{PLS1*}$-mEGFP::HIS3* | This study |
| PHY10037 | (SK1) *MAT***a** *ura3 leu2 trp1 his3 lys2 hoΔ::LYS2 HRR25-mEGFP::NAT*/(BY) *MATα his3Δ1 leu2Δ0 lys2Δ0 ura3Δ0 HRR25-mEGFP::NAT can1Δ::STE2pro-Sp_HIS5* | This study |
| PHY10041 | (SK1) *MAT***a** *ura3 leu2 trp1 his3 lys2 hoΔ::LYS2 HRR25$^{PLS1*}$-mEGFP::NAT*/(BY) *MATα his3Δ1 leu2Δ0 lys2Δ0 ura3Δ0 HRR25$^{PLS1*}$-mEGFP::NAT can1Δ::STE2pro-Sp_HIS5* | This study |
| PHY9593 | (BY) *MAT***a** *his3Δ1 leu2Δ0 met15Δ0 ura3Δ0 HRR25-mEGFP::HIS3 EDC3-mCherry::LEU2*/(SK1) *MATα ura3 leu2 trp1 his3 arg4 lys2 hoΔ::LYS2 rme1Δ::LEU2 hrr25::TRP1* | This study |
| PHY10677 | (BY) *MAT***a** *his3Δ1 leu2Δ0 met15Δ0 ura3Δ0 HRR25-mEGFP::HIS3 MAM1-13Myc::LEU2*/(SK1) *MATα ura3 leu2 trp1 his3 arg4 lys2 hoΔ::LYS2 rme1Δ::LEU2 HRR25-mEGFP::HIS3 MAM1-13Myc::TRP1* | This study |
| PHY10681 | (BY) *MAT***a** *his3Δ1 leu2Δ0 met15Δ0 ura3Δ0 HRR25$^{PLS1*}$-mEGFP::HIS3 MAM1-13Myc::LEU2*/(SK1) *MATα ura3 leu2 trp1 his3 arg4 lys2 hoΔ::LYS2 rme1Δ::LEU2 HRR25$^{PLS1*}$-mEGFP::HIS3 MAM1-13Myc::TRP1* | This study |
| PHY6238 | (BY) *MAT***a** *his3Δ1 leu2Δ0 met15Δ0 ura3Δ0 HRR25-mEGFP::HIS3 EDC3-mCherry::LEU2* | 31 |
| PHY6262 | (BY) *MAT***a** *his3Δ1 leu2Δ0 met15Δ0 ura3Δ0 HRR25$^{AS}$-mEGFP::HIS3 EDC3-mCherry::LEU2* | 31 |
| PHY7442 | (BY) *MAT***a** *his3Δ1 leu2Δ0 met15Δ0 ura3Δ0 HRR25$^{PLS1*}$-mEGFP::HIS3 EDC3-mCherry::LEU2* | 31 |
| PHY10119 | (BY) *MAT***a** *his3Δ1 leu2Δ0 met15Δ0 ura3Δ0 HRR25$^{ZO}$-mEGFP::HIS3, Edc3-mCherry::LEU2* | This study |

[a]The diploids are listed so as to show the genotypes of the starting haploid strains, including whether they were in the BY or SK1 genetic backgrounds. The loci of note in each strain are indicated in boldface.

Unless otherwise noted, the diploid strains used were all isogenic derivatives generated by crossing a BY4741*a* haploid strain with an SK1$\alpha$ haploid. Strains of the latter lineage exhibit an exceptionally high level of sporulation, and the hybrid diploids were found to sporulate much more efficiently than BY/BY-based diploids (57, 58). In each case, we introduced the desired genetic alterations into one or both of these parental strains as required and then crossed the two haploid products to generate the final diploid strains. The *pat1*Δ/*pat1*Δ strain, PHY8837, was generated by crossing BY4741*a* and BY4742$\alpha$ derivatives that contained the indicated deletion allele of the *PAT1* locus. The *dcp2*Δ/*dcp2*Δ strain, PHY8694, was constructed by crossing BY4741 *dcp2*Δ with a *dcp2*Δ strain, Y4835$\alpha$, that was generously provided by Roy Parker. All tagged proteins were expressed from their respective endogenous loci with the exception of the construct used for the Hrr25$^{PLS1*}$ overexpression study, where expression was from the copper-inducible promoter of the *CUP1* gene. This overexpression plasmid, pPHY4332, was constructed in the pRS416 vector (59).

**Sporulation protocol.** Sporulation was induced in diploid strains as described previously (60, 61). Briefly, diploid strains were grown to mid-log phase in rich medium (1% yeast extract, 2% peptone, 50 mg/liter adenine, 2% glucose [YPAD]), transferred to presporulation medium (yeast extract-peptone-adenine supplemented with 1% potassium acetate), and incubated with vigorous aeration (200 rpm) for 12 to 16 h. The cells were harvested when the optical density at 600 nm ($OD_{600}$) of the culture was approximately 1.6 and were then transferred to sporulation medium (SPM; 1% potassium acetate) and incubated with vigorous aeration for up to 24 h. During this time, the concentration of cells was carefully monitored and kept under $1.1 \times 10^7$ cells/ml to avoid overcrowding.

**Microscopy and data analysis.** For the analysis of sporulation, cells with the indicated genetic background were collected by centrifugation 24 h after switching to sporulation medium. Cells were fixed with 70% ethanol for 5 min and washed twice with deionized water. The cells were resuspended in 50 $\mu$l double-distilled $H_2O$ with 2 $\mu$g/ml 4′,6-diamidino-2-phenylindole (DAPI) and spotted onto a 3% agarose pad. Spores were observed using an inverted microscope (Eclipse Ti; Nikon) equipped with an Andor Zyla digital camera, Nikon HC filters, and a 100×/1.45-numeric-aperture (NA) Plan-Apo objective lens (Nikon). The efficiency of sporulation was calculated according to an equation used previously by Knop and his colleagues and other researchers (62): sporulation efficiency = [(% tetrads × 4) + (% triads × 3) + (% dyads × 2) + % monads]/4.

For the analysis of P-bodies, yeast strains expressing the indicated fusion proteins were subjected to the above-described sporulation regimen. Cells were collected at the indicated time points, and P-bodies were observed as described previously (31, 44). Most images were taken with the inverted fluorescence microscope mentioned above, with the exception of the colocalization analyses. For the latter, images were taken with a spinning disk confocal system (UltraVIEW Vox CSUX1 system; PerkinElmer) with 405-, 488-, and 561-nm solid-state lasers and dual-back thinned electron-modifying charge-coupled device cameras (C9100-13; Hamamatsu Photonics) using a Nikon Ti-E inverted microscope, without binning, under single camera mode with a 100×/1.4-NA Plan-Apo objective lens (Nikon). Images were taken with the NIS-Elements AR (Nikon) and Volocity (PerkinElmer) software packages and analyzed with ImageJ software (National Institutes of Health). For the microscopy, we typically performed each experiment in triplicate and analyzed at least 100 cells in each replicate. The error bars on the graphs depicting the quantitation of these data indicate the standard deviations unless otherwise noted. To assess Hrr25 localization at the different stages of meiosis, we used fluorescence microscopy to examine premeiotic cells (2 h in SPM), cells undergoing meiotic divisions I and II (8 h in SPM), and postmeiotic cells (24 h in SPM). The degree of colocalization with an Edc3-mCh reporter was determined at each stage in at least 30 individual cells for two independent isolates of the tagged strain.

**Sporulation plating assay.** For the sporulation plating assay, we constructed isogenic *HRR25*$^{WT}$/*HRR25*$^{WT}$ and *hrr25*$^{PLS1*}$/*hrr25*$^{PLS1*}$ diploid strains. These strains carry one copy of the *his5*$^{+}$ gene from *S. pombe* under the control of the *STE2* gene promoter that is active only in *MAT***a** haploid cells. The starting strain is homozygous for a deletion of the *HIS3* locus, and the *S. pombe his5*$^{+}$ gene can complement this *his3*Δ mutation (50). Thus, *MAT***a** haploid cells produced as a result of meiosis and sporulation are able to grow on minimal medium lacking histidine. Neither *MAT*$\alpha$ haploid nor **a**/$\alpha$ diploid cells are able to grow on this selective medium. The number of resulting colonies on medium lacking histidine (histidine-minus medium) therefore serves as a measure of the sporulation efficiency of the starting diploid strain. For these studies, sporulation was induced for 24 h as described above, and cells were then collected by centrifugation. These cells were resuspended in water at a final concentration of 10 $OD_{600}$ equivalents/ml, and 5 $\mu$l of this cell suspension, and 5-fold serial dilutions thereafter, were plated onto both selective (SCD His-minus) and control (YPAD) media. The colonies were counted after 2 to 3 days of growth at 30°C. Diploid cells were also collected before sporulation and plated in the same manner. One advantage of this assay is that it determines the fraction of viable meiotic products resulting from the induction of the sporulation process.

**Protein analysis.** Protein samples for Western blotting were prepared with a trichloroacetic acid precipitation method described previously (63, 64). Proteins were separated on SDS-polyacrylamide gels, and Western blotting was performed as described above. The mEGFP epitope tag and Pgk1 were detected with the appropriate primary and secondary antibodies. The SuperSignal chemiluminescent substrate (Pierce) was subsequently used to detect the reactive bands. Coimmunoprecipitation assays were performed as described previously (31, 65).

## ACKNOWLEDGMENTS

We thank Charlie Boone, Aaron Neiman, and Jeremy Thorner for reagents used in this study and members of the Herman laboratory for helpful discussions and comments on the manuscript.

This work was supported by grants GM101191 and GM065227 from the National Institutes of Health to P.K.H. and a graduate student fellowship from the Pelotonia Fellowship Program to B.Z.

## REFERENCES

1. Hyman AA, Weber CA, Julicher F. 2014. Liquid-liquid phase separation in biology. Annu Rev Cell Dev Biol 30:39–58. https://doi.org/10.1146/annurev-cellbio-100913-013325.
2. Aguzzi A, Altmeyer M. 2016. Phase separation: linking cellular compartmentalization to disease. Trends Cell Biol 26:547–558. https://doi.org/10.1016/j.tcb.2016.03.004.
3. Brangwynne CP, Mitchison TJ, Hyman AA. 2011. Active liquid-like behavior of nucleoli determines their size and shape in Xenopus laevis oocytes. Proc Natl Acad Sci U S A 108:4334–4339. https://doi.org/10.1073/pnas.1017150108.
4. Buchan JR. 2014. mRNP granules. Assembly, function, and connections with disease. RNA Biol 11:1019–1030.
5. Li YR, King OD, Shorter J, Gitler AD. 2013. Stress granules as crucibles of ALS pathogenesis. J Cell Biol 201:361–372. https://doi.org/10.1083/jcb.201302044.
6. Patel A, Lee HO, Jawerth L, Maharana S, Jahnel M, Hein MY, Stoynov S, Mahamid J, Saha S, Franzmann TM, Pozniakovski A, Poser I, Maghelli N, Royer LA, Weigert M, Myers EW, Grill S, Drechsel D, Hyman AA, Alberti S. 2015. A liquid-to-solid phase transition of the ALS protein FUS accelerated by disease mutation. Cell 162:1066–1077. https://doi.org/10.1016/j.cell.2015.07.047.
7. Aulas A, Vande Velde C. 2015. Alterations in stress granule dynamics driven by TDP-43 and FUS: a link to pathological inclusions in ALS? Front Cell Neurosci 9:423. https://doi.org/10.3389/fncel.2015.00423.

8. Luo Y, Na Z, Slavoff SA. 2018. P-bodies: composition, properties, and functions. Biochemistry 57:2424–2431. https://doi.org/10.1021/acs.biochem.7b01162.
9. Jain S, Parker R. 2013. The discovery and analysis of P bodies. Adv Exp Med Biol 768:23–43. https://doi.org/10.1007/978-1-4614-5107-5_3.
10. Bashkirov VI, Scherthan H, Solinger JA, Buerstedde JM, Heyer WD. 1997. A mouse cytoplasmic exoribonuclease (mXRN1p) with preference for G4 tetraplex substrates. J Cell Biol 136:761–773. https://doi.org/10.1083/jcb.136.4.761.
11. Cougot N, Babajko S, Seraphin B. 2004. Cytoplasmic foci are sites of mRNA decay in human cells. J Cell Biol 165:31–40. https://doi.org/10.1083/jcb.200309008.
12. Ingelfinger D, Arndt-Jovin DJ, Luhrmann R, Achsel T. 2002. The human LSm1-7 proteins colocalize with the mRNA-degrading enzymes Dcp1/2 and Xrnl in distinct cytoplasmic foci. RNA 8:1489–1501.
13. Sheth U, Parker R. 2003. Decapping and decay of messenger RNA occur in cytoplasmic processing bodies. Science 300:805–808. https://doi.org/10.1126/science.1082320.
14. van Dijk E, Cougot N, Meyer S, Babajko S, Wahle E, Seraphin B. 2002. Human Dcp2: a catalytically active mRNA decapping enzyme located in specific cytoplasmic structures. EMBO J 21:6915–6924. https://doi.org/10.1093/emboj/cdf678.
15. Balagopal V, Parker R. 2009. Polysomes, P bodies and stress granules: states and fates of eukaryotic mRNAs. Curr Opin Cell Biol 21:403–408. https://doi.org/10.1016/j.ceb.2009.03.005.
16. Eulalio A, Behm-Ansmant I, Izaurralde E. 2007. P bodies: at the crossroads of post-transcriptional pathways. Nat Rev Mol Cell Biol 8:9–22. https://doi.org/10.1038/nrm2080.
17. Decker CJ, Teixeira D, Parker R. 2007. Edc3p and a glutamine/asparagine-rich domain of Lsm4p function in processing body assembly in Saccharomyces cerevisiae. J Cell Biol 179:437–449. https://doi.org/10.1083/jcb.200704147.
18. Eulalio A, Behm-Ansmant I, Schweizer D, Izaurralde E. 2007. P-body formation is a consequence, not the cause, of RNA-mediated gene silencing. Mol Cell Biol 27:3970–3981. https://doi.org/10.1128/MCB.00128-07.
19. Stoecklin G, Mayo T, Anderson P. 2006. ARE-mRNA degradation requires the 5′-3′ decay pathway. EMBO Rep 7:72–77. https://doi.org/10.1038/sj.embor.7400572.
20. Huch S, Nissan T. 2017. An mRNA decapping mutant deficient in P body assembly limits mRNA stabilization in response to osmotic stress. Sci Rep 7:44395. https://doi.org/10.1038/srep44395.
21. Hubstenberger A, Courel M, Benard M, Souquere S, Ernoult-Lange M, Chouaib R, Yi Z, Morlot JB, Munier A, Fradet M, Daunesse M, Bertrand E, Pierron G, Mozziconacci J, Kress M, Weil D. 2017. P-body purification reveals the condensation of repressed mRNA regulons. Mol Cell 68:144–157. https://doi.org/10.1016/j.molcel.2017.09.003.
22. Arimoto K, Fukuda H, Imajoh-Ohmi S, Saito H, Takekawa M. 2008. Formation of stress granules inhibits apoptosis by suppressing stress-responsive MAPK pathways. Nat Cell Biol 10:1324–1332. https://doi.org/10.1038/ncb1791.
23. Kozubowski L, Aboobakar EF, Cardenas ME, Heitman J. 2011. Calcineurin colocalizes with P-bodies and stress granules during thermal stress in Cryptococcus neoformans. Eukaryot Cell 10:1396–1402. https://doi.org/10.1128/EC.05087-11.
24. Mitchell SF, Jain S, She M, Parker R. 2013. Global analysis of yeast mRNPs. Nat Struct Mol Biol 20:127–133. https://doi.org/10.1038/nsmb.2468.
25. Shah KH, Nostramo R, Zhang B, Varia SN, Klett BM, Herman PK. 2014. Protein kinases are associated with multiple, distinct cytoplasmic granules in quiescent yeast cells. Genetics 198:1495–1512. https://doi.org/10.1534/genetics.114.172031.
26. Takahara T, Maeda T. 2012. Transient sequestration of TORC1 into stress granules during heat stress. Mol Cell 47:242–252. https://doi.org/10.1016/j.molcel.2012.05.019.
27. Tudisca V, Recouvreux V, Moreno S, Boy-Marcotte E, Jacquet M, Portela P. 2010. Differential localization to cytoplasm, nucleus or P-bodies of yeast PKA subunits under different growth conditions. Eur J Cell Biol 89:339–348. https://doi.org/10.1016/j.ejcb.2009.08.005.
28. Wippich F, Bodenmiller B, Trajkovska MG, Wanka S, Aebersold R, Pelkmans L. 2013. Dual specificity kinase DYRK3 couples stress granule condensation/dissolution to mTORC1 signaling. Cell 152:791–805. https://doi.org/10.1016/j.cell.2013.01.033.
29. Thedieck K, Holzwarth B, Prentzell MT, Boehlke C, Klasener K, Ruf S, Sonntag AG, Maerz L, Grellscheid SN, Kremmer E, Nitschke R, Kuehn EW, Jonker JW, Groen AK, Reth M, Hall MN, Baumeister R. 2013. Inhibition of mTORC1 by astrin and stress granules prevents apoptosis in cancer cells. Cell 154:859–874. https://doi.org/10.1016/j.cell.2013.07.031.
30. Kedersha N, Ivanov P, Anderson P. 2013. Stress granules and cell signaling: more than just a passing phase? Trends Biochem Sci 38:494–506. https://doi.org/10.1016/j.tibs.2013.07.004.
31. Zhang B, Shi Q, Varia SN, Xing S, Klett BM, Cook LA, Herman PK. 2016. The activity-dependent regulation of protein kinase stability by the localization to P-bodies. Genetics 203:1191–1202. https://doi.org/10.1534/genetics.116.187419.
32. DeMaggio AJ, Lindberg RA, Hunter T, Hoekstra MF. 1992. The budding yeast HRR25 gene product is a casein kinase I isoform. Proc Natl Acad Sci U S A 89:7008–7012. https://doi.org/10.1073/pnas.89.15.7008.
33. Hoekstra MF, Liskay RM, Ou AC, DeMaggio AJ, Burbee DG, Heffron F. 1991. HRR25, a putative protein kinase from budding yeast: association with repair of damaged DNA. Science 253:1031–1034. https://doi.org/10.1126/science.1887218.
34. Petronczki M, Matos J, Mori S, Gregan J, Bogdanova A, Schwickart M, Mechtler K, Shirahige K, Zachariae W, Nasmyth K. 2006. Monopolar attachment of sister kinetochores at meiosis I requires casein kinase 1. Cell 126:1049–1064. https://doi.org/10.1016/j.cell.2006.07.029.
35. Schafer T, Maco B, Petfalski E, Tollervey D, Bottcher B, Aebi U, Hurt E. 2006. Hrr25-dependent phosphorylation state regulates organization of the pre-40S subunit. Nature 441:651–655. https://doi.org/10.1038/nature04840.
36. Ray P, Basu U, Ray A, Majumdar R, Deng H, Maitra U. 2008. The Saccharomyces cerevisiae 60 S ribosome biogenesis factor Tif6p is regulated by Hrr25p-mediated phosphorylation. J Biol Chem 283:9681–9691. https://doi.org/10.1074/jbc.M710294200.
37. Grozav AG, Chikamori K, Kozuki T, Grabowski DR, Bukowski RM, Willard B, Kinter M, Andersen AH, Ganapathi R, Ganapathi MK. 2009. Casein kinase I delta/epsilon phosphorylates topoisomerase IIalpha at serine-1106 and modulates DNA cleavage activity. Nucleic Acids Res 37:382–392. https://doi.org/10.1093/nar/gkn934.
38. Biswas A, Mukherjee S, Das S, Shields D, Chow CW, Maitra U. 2011. Opposing action of casein kinase 1 and calcineurin in nucleo-cytoplasmic shuttling of mammalian translation initiation factor eIF6. J Biol Chem 286:3129–3138. https://doi.org/10.1074/jbc.M110.188565.
39. Lord C, Bhandari D, Menon S, Ghassemian M, Nycz D, Hay J, Ghosh P, Ferro-Novick S. 2011. Sequential interactions with Sec23 control the direction of vesicle traffic. Nature 473:181–186. https://doi.org/10.1038/nature09969.
40. Arguello-Miranda O, Zagoriy I, Mengoli V, Rojas J, Jonak K, Oz T, Graf P, Zachariae W. 2017. Casein kinase 1 coordinates cohesin cleavage, gametogenesis, and exit from M phase in meiosis II. Dev Cell 40:37–52. https://doi.org/10.1016/j.devcel.2016.11.021.
41. Peng Y, Grassart A, Lu R, Wong CC, Yates J, III, Barnes G, Drubin DG. 2015. Casein kinase 1 promotes initiation of clathrin-mediated endocytosis. Dev Cell 32:231–240. https://doi.org/10.1016/j.devcel.2014.11.014.
42. Ghalei H, Schaub FX, Doherty JR, Noguchi Y, Roush WR, Cleveland JL, Stroupe ME, Karbstein K. 2015. Hrr25/CK1delta-directed release of Ltv1 from pre-40S ribosomes is necessary for ribosome assembly and cell growth. J Cell Biol 208:745–759. https://doi.org/10.1083/jcb.201409056.
43. Neiman AM. 2011. Sporulation in the budding yeast Saccharomyces cerevisiae. Genetics 189:737–765. https://doi.org/10.1534/genetics.111.127126.
44. Shah KH, Zhang B, Ramachandran V, Herman PK. 2013. Processing body and stress granule assembly occur by independent and differentially regulated pathways in Saccharomyces cerevisiae. Genetics 193:109–123. https://doi.org/10.1534/genetics.112.146993.
45. Teixeira D, Sheth U, Valencia-Sanchez MA, Brengues M, Parker R. 2005. Processing bodies require RNA for assembly and contain nontranslating mRNAs. RNA 11:371–382. https://doi.org/10.1261/rna.7258505.
46. Ramachandran V, Shah KH, Herman PK. 2011. The cAMP-dependent protein kinase signaling pathway is a key regulator of P body foci formation. Mol Cell 43:973–981. https://doi.org/10.1016/j.molcel.2011.06.032.
47. Teixeira D, Parker R. 2007. Analysis of P-body assembly in Saccharomyces cerevisiae. Mol Biol Cell 18:2274–2287. https://doi.org/10.1091/mbc.e07-03-0199.
48. Pilkington GR, Parker R. 2008. Pat1 contains distinct functional domains that promote P-body assembly and activation of decapping. Mol Cell Biol 28:1298–1312. https://doi.org/10.1128/MCB.00936-07.
49. Lusk CP, Waller DD, Makhnevych T, Dienemann A, Whiteway M, Thomas

DY, Wozniak RW. 2007. Nup53p is a target of two mitotic kinases, Cdk1p and Hrr25p. Traffic 8:647–660. https://doi.org/10.1111/j.1600-0854.2007.00559.x.
50. Kuzmin E, Sharifpoor S, Baryshnikova A, Costanzo M, Myers CL, Andrews BJ, Boone C. 2014. Synthetic genetic array analysis for global mapping of genetic networks in yeast. Methods Mol Biol 1205:143–168. https://doi.org/10.1007/978-1-4939-1363-3_10.
51. Ho Y, Mason S, Kobayashi R, Hoekstra M, Andrews B. 1997. Role of the casein kinase I isoform, Hrr25, and the cell cycle-regulatory transcription factor, SBF, in the transcriptional response to DNA damage in Saccharomyces cerevisiae. Proc Natl Acad Sci U S A 94:581–586. https://doi.org/10.1073/pnas.94.2.581.
52. Lee MS, Joo JH, Kim K. 2017. Roles of budding yeast Hrr25 in recombination and sporulation. J Microbiol Biotechnol 27:1198–1203.
53. Corbett KD, Harrison SC. 2012. Molecular architecture of the yeast monopolin complex. Cell Rep 1:583–589. https://doi.org/10.1016/j.celrep.2012.05.012.
54. Sarkar S, Shenoy RT, Dalgaard JZ, Newnham L, Hoffmann E, Millar JB, Arumugam P. 2013. Monopolin subunit Csm1 associates with MIND complex to establish monopolar attachment of sister kinetochores at meiosis I. PLoS Genet 9:e1003610. https://doi.org/10.1371/journal.pgen.1003610.
55. Ye Q, Ur SN, Su TY, Corbett KD. 2016. Structure of the Saccharomyces cerevisiae Hrr25:Mam1 monopolin subcomplex reveals a novel kinase regulator. EMBO J 35:2139–2151. https://doi.org/10.15252/embj.201694082.
56. Longtine MS, McKenzie A, III, Demarini DJ, Shah NG, Wach A, Brachat A, Philippsen P, Pringle JR. 1998. Additional modules for versatile and economical PCR-based gene deletion and modification in Saccharomyces cerevisiae. Yeast 14:953–961. https://doi.org/10.1002/(SICI)1097-0061(199807)14:10<953::AID-YEA293>3.0.CO;2-U.
57. Kane SM, Roth R. 1974. Carbohydrate metabolism during ascospore development in yeast. J Bacteriol 118:8–14.
58. Herman PK, Rine J. 1997. Yeast spore germination: a requirement for Ras protein activity during re-entry into the cell cycle. EMBO J 16:6171–6181. https://doi.org/10.1093/emboj/16.20.6171.
59. Sikorski RS, Hieter P. 1989. A system of shuttle vectors and yeast host strains designed for efficient manipulation of DNA in Saccharomyces cerevisiae. Genetics 122:19–27.
60. Borner GV, Cha RS. 2015. Induction and analysis of synchronous meiotic yeast cultures. Cold Spring Harb Protoc 2015:908–913. https://doi.org/10.1101/pdb.prot085035.
61. Nakanishi H, Suda Y, Neiman AM. 2007. Erv14 family cargo receptors are necessary for ER exit during sporulation in Saccharomyces cerevisiae. J Cell Sci 120:908–916. https://doi.org/10.1242/jcs.03405.
62. Taxis C, Keller P, Kavagiou Z, Jensen LJ, Colombelli J, Bork P, Stelzer EH, Knop M. 2005. Spore number control and breeding in Saccharomyces cerevisiae: a key role for a self-organizing system. J Cell Biol 171:627–640. https://doi.org/10.1083/jcb.200507168.
63. Budovskaya YV, Hama H, DeWald DB, Herman PK. 2002. The C terminus of the Vps34p phosphoinositide 3-kinase is necessary and sufficient for the interaction with the Vps15p protein kinase. J Biol Chem 277:287–294. https://doi.org/10.1074/jbc.M109263200.
64. Budovskaya YV, Stephan JS, Reggiori F, Klionsky DJ, Herman PK. 2004. The Ras/cAMP-dependent protein kinase signaling pathway regulates an early step of the autophagy process in Saccharomyces cerevisiae. J Biol Chem 279:20663–20671. https://doi.org/10.1074/jbc.M400272200.
65. Deminoff SJ, Ramachandran V, Herman PK. 2009. Distal recognition sites in substrates are required for efficient phosphorylation by the cAMP-dependent protein kinase. Genetics 182:529–539. https://doi.org/10.1534/genetics.109.102178.